Electronic properties of vacancies in bilayer *graphane*

R. E. Mapasha[a,*], E. Igumbor[b], N.F. Andriambelaza[a], N. Chetty[a,c]

[a] *Department of Physics, University of Pretoria, Hatfield campus, Pretoria 0002, RSA*
[b] *School of Interdisciplinary Research and Graduate Studies, University of South Africa, UNISA 0003, Preller Street, Pretoria, RSA*
[c] *National Institute for Theoretical Physics, Johannesburg 2000, RSA*

Abstract

We have performed the *ab initio* hybrid density functional theory (DFT) calculations to investigate the electronic structure of various neutral and charged vacancies (V_H, V_{CH}, V_C, V_{C-CH} and V_{C-C}) in a diamond-like bilayer *graphane*. In the neutral state, the identified vacancies create the energetically unfavorable dangling bonds which are significantly stabilize by electron ejection (+1 state) mechanism. The studied vacancies introduce the electronic states within the band gap, which are either metallic or semiconducting in nature. The metallic vacancies posses a magnetic moment of 1.00 μ_B. The charge states modulation alters the electronic character of the vacancies and suppresses the induced magnetic moment. Our study demonstrates that the vacancies in a diamond-like bilayer *graphane* structure could have potential applications in nanoelectronics and band gap related energy storage devices.

Keywords: Diamond-like bilayer *graphane*, Density Functional Theory, Vacancies, Charge states, Electronic characters

1. Introduction

The idea of graphene derivatives (*graphane* [1, 2], flourographene [3], chlorographene [4]) became popular when opening the band gap in graphene received a lot of research attention. Graphene has the peculiar charge carriers behaving as the massless Dirac fermions in the reciprocal space, exotic quantum Hall effect, the charge carriers have ballistic mobility at room temperatures, high specific surface area and semi-metallic in nature [5, 6, 7, 8]. Theoretically, a single layer *graphane* system should be made of the hydrogen

*Corresponding author
Email address: edwin.mapasha@up.ac.za (R. E. Mapasha)

(H) atoms attached to the two distinct carbon (C) sublattices of graphene plane in an alternative manner [1]. Currently, the hydrogenation mechanism is widely applied to various two dimensional (2D) materials such as hexagonal boron nitride, phosphorene etc. to alter their physical properties [9, 10, 11]. The most popular single layer *graphane* samples were obtained from the H plasma exposure to graphene at relatively low temperature [2]. Although *graphane* samples are inherently two dimensional structurally, they posses a tetragonal network with sp^3 hybridized bonds around the C atoms, and are thermodynamically stable at room temperatures [2].

Experimental characterization of the single layer *graphane* samples conducted using transmission electron microscopy (TEM) [2] reveals an insulating character, in agreement, *ab initio* previous studies report the relatively wide band gap depending on the exchange correlation functional used [1, 12, 13, 14]. Based on the noted properties, *graphane* seems to be suitable for various electronic and energy storage device applications. Bilayer *graphane* proposed by Leenaerts et al. [15] has a fascinating bonding network because the process of hydrogenation on the bilayer graphene structure occurs only on the outer sides of the surfaces. One C sublattice is hydrogenated while the other C sublattice is with bare H atom. Due to this structural arrangement, there is enforcement on the bare H carbon atoms to bend inwards on both layers forming out of plane C-C covalent bonds overcoming the intrinsic van der Waals bonding, showing a diamond-like bilayer *graphane* network [15, 16, 17].

Although the single layer and bilayer *graphane* systems have similar electronic characters [15], the later is more robust due to bilayer network bonding [18, 19]. During the structural characterization of single layer *graphane* using experimental methods, the atomic vacancies were noted [2], and were attributed to the effects of plasma damage and due to this, the induced mid-gap states were reported. Defects such as vacancies and substitutional impurities play a pivotal role in determining the new applications of the material systems, and they usually affect the electronic and optical properties. Vacancies in single layer *graphane* create the unpaired electrons (dangling bonds) responsible for newly added localized states within the band gap [2]. The ability to control the defect induced properties is important for the device operations. In order to achieve this, various theoretical studies were conducted to study the various properties of missing hydrogen V_H vacancy and hydrogen-carbon vacancy pair V_{CH} in a single layer *graphane* [20, 21, 22]. In bilayer *graphane*, more unique vacancies are expected to exist and worth to be characterized. The magnetic moment of 1.00 μ_B in both systems was recorded attributing to the difference in the induced electronic spins. This induced magnetic moment is suppressed through hydrogena-

tion of carbon atoms possesing dangling bonds [22] and also through radical molecule adsorption [23]. The latter method was also considered in the studies of other 2D materials containing vacancies [24]. A lithium adatom and charge states modulation stabilize the vacancy and also increases the magnetic moment [25].

In this work, different types of vacancies such as the hydrogen vacancy (V_H), carbon vacancy (V_C) and hydrogen-carbon pair vacancy V_{CH}, as well as the nearest neighbor carbon-carbon pair divacancy (V_{C-C}) are created in a diamond-like bilayer *graphane*, and studied using a hybrid density functional approach. The thermodynamic stability, transition levels, vacancy induced electronic properties and magnetic moments are evaluated. We also examine the influence of charge states modulation on the vacancy induced electronic states.

2. Computational details

The electronic structure of the identified vacancies has been investigated using the calculations based on the hybrid density functional theory (DFT) approach implemented within the Vienna *ab initio* simulation package (VASP) code [26]. All the calculations were performed by replacing the core-electron interactions with the pseudopotentials (with $2s^2 2p^2$ and $1s^1$ valence electrons of the C and H atoms, respectively) derived from the projector augmented wave (PAW) methods [27]. The effects of exchange correlation interactions were addressed using the screened hybrid exchange correlation functional developed by Heyd, Scuseria, and Ernzerhof (HSE06 functional) flavour [28]. This method has been praised to correctly predict the band gap and defect transition levels. All the calculations were performed without imposing any spin restriction.

The Monkhorst-Pack scheme [29] was used to generate the $2\times2\times1$ k-point meshes suitable for sampling the Brillouin zone of 6×6 supercell size with isolated vacancy defect. We used 500 eV energy cut-off to expand the plane wavefunctions. The calculations were allowed to run until the forces between the atoms are less than 0.01 eVÅ^{-1}, using the Hellman-Feynman theorem. We allowed the total energy of the vacancies to converge to within 10^{-7} eV during the self-consistent field calculations. In the first-principles calculations, the periodic boundary conditions plays a significant role, and the z-axis was set to 20 Å to eliminate the fictitious periodic image interactions.

To understand the thermodynamic stability of the diamond-like vacancies in the various charge state q, the formation energies were calculated using this equation,

$$E^q_{form}(V) = E^q_{tot}(V) - E_{tot}(G) - \sum_i n_i\mu_i + q(E_F + \epsilon_v) + E_{corr}. \quad (1)$$

The terms $E^q_{tot}(V_{CH})$ and $E_{tot}(G)$ are the total energies of 6×6 supercell size diamond-like bilayer *graphane* with vacancy and without vacancy respectively, in various charge states (q). The chemical potentials of H and C atoms are the total energies of isolated H_2 dimer placed in a large cubic cell of lattice constants a=b=c=20 Å and graphene layer respectively, and are represented by μ_i in equation 1. n_i is the number of atomic H or C atoms. E_F is the the Fermi level position which is an electronic chemical potential found in the electron reservoir. The ϵ_v is the energy level valence band maximum (VBM) of a pristine diamond-like *graphane* system. E_{corr} term is the supercell corrections term for two (2D) dimensional systems accounting for the elimination of effect of fictitious electrostatic interactions of the charged vacancy with its periodic images, developed from Refs [30, 31].

3. Results and discussion

3.1. Vacancy configurations studied

In this work, the physical properties of the various vacancies in a 6×6 supercell of a diamond-like bilayer *graphane* structure are investigated. Fig. 1(b-f) presents the vacancy configurations studied in this paper. The most popular studied vacancy is the missing H in bilayer *graphane* denoted as V_H (Fig. 1(b)) followed by hydrogen-carbon pair vacancy denoted as V_{CH} (Fig. 1(c)). The other vacancies which cannot exist in a single layer *graphane* but possible in diamond-like bilayer *graphane* are carbon vacancy (Fig. 1(d)) denoted as V_C, divacancy constituted by the nearest neighbor CH pair with C (V_{CH-C}) (Fig. 1(e)) and lastly divacancy constituted by the nearest neighbor C atoms from the adjacent layers denoted as V_{C-C} (Fig. 1(f)).

3.2. The energetics of the vacancies

For thermodynamic stability analysis, Table 1 summarizes the calculated formation energies of each vacancy in diamond-like in the various charge states (-1,0,+1). When the position of Fermi level is at 0.00 eV calculated using equation 1, the formation energy of V_H vacancy at a neutral state is lowest compared to other considered vacancies ($E_{form}(V_H) < E_{form}(V_{C-CH}) < E_{form}(V_{CH}) < E_{form}(V_{C-C}) < E_{form}(V_C)$), calculated at the same accuracy level. As expected to be endothermic formation, V_H can be achieved at a reasonable amount of energy compared to its single layer counterpart [17]. Evidently, our formation energy for V_H is lower than those reported in

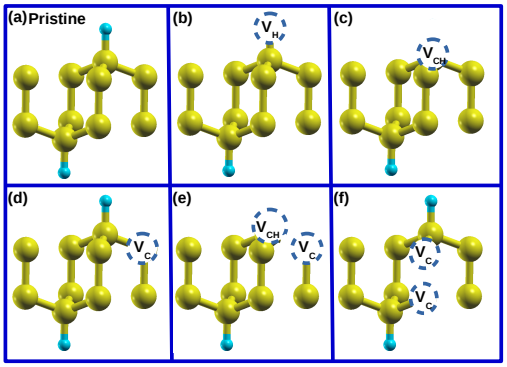

Figure 1: (a) The unit cell of pristine bilayer *graphane*. Different vacancies (b) V_H, (c) V_{CH} and (d) V_C and divacancies (e) V_{C-CH} and (f)V_{C-C} in bilayer *graphane*. The C and H host atoms are indicated by the Yellow and light green spheres, respectively.

Refs [20, 32], for single layer *graphane*. Although the V_H vacancy can occur unintentional during the plasma hydrogenation of bilayer *graphane*, it can be created as a result of the application of electric field since it was achieved in a single layer *graphane* monolayer [20].

Apart from V_H vacancy, all other vacancies shown in Fig 1 involve the removal of one or two C atoms as well as the C-H pair which will require high amount of energy to create. Nonetheless, these vacancies can be achieved using experimental pathways such as high-energy ion beams, the method used to create vacancies in a single layer graphene[33]. The reasonable amount of formation energy of 2.73 eV from divacancy V_{C-CH} could be attributed to the possible structural reconstruction on the top layer leading to the formation of 5-8-5 ringed defect structure during the structural relaxation noted in a single layer graphane[22].

Table 1: The calculated formation energies (eV) of the different vacancies identified from bilayer *graphane* evaluated in various charge states. The bold value indicates the most stable vacancy at each charge state. The asterisk $\star$ indicates results from single layer *graphane*. The formation energy of bilayer *graphane* is approximately $-0.50\ eV$ [15].

Vacancies	-1	0	$+1$
V_H	$\mathbf{6.69}(4.91)^{a\star}$	$\mathbf{1.69}(2.23)^{a\star}(4.79)^{b\star}(3.65)^{c\star}$	$\mathbf{-0.62}(1.51)^{a\star}$
V_{CH}	9.37 $(9.52)^{d\star}$	3.89 $(6.01)^{d\star}$	0.29 $(3.77)^{d\star}$
V_C	10.36	5.32	2.57
V_{C-CH}	6.84	2.73	0.31
V_{C-C}	7.04	4.13	1.95

^{a}Ref[17], ^{b}Ref[20], ^{c}Ref[32] and ^{d}Ref[25]

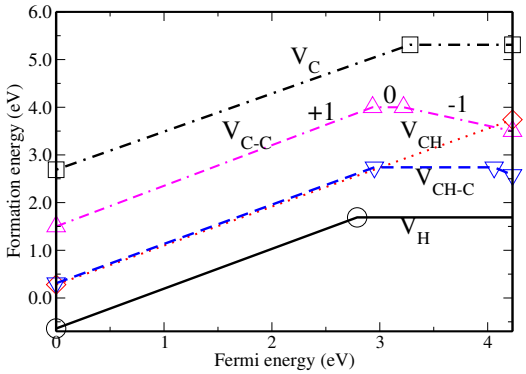

Figure 2: The calculated formation energies of the various vacancies in their nominal charge states (-1, 0, +1) within a band gap as a function of the Fermi level. The slope of each graph corresponds to the charge state. Each point where the two plots intersect yield the thermodynamic transition levels.

Ejection of an electron (+1 charge state) from these type of vacancies lowers the energy of the system significantly compared to neutral calculations and follows this formation energy sequence: $E_{form}(V_H) < E_{form}(V_{CH}) < E_{form}(V_{C-CH}) < E_{form}(V_{C-C}) < E_{form}(V_C)$. It is evident that creating the vacancies in a bilayer *graphane* system leaves energetically unfavorable dangling bonds which can be reduced through H passivation [22] or electron ejection. It is noted that V_{CH} vacancy overlaps with V_{C-CH} at +1 charge states compared to neutral charge state, suggesting that the thermodynamic stability of a vacancy configuration over the other is merely charge state dependent. Addition of an electron into these vacancy configurations substantially increases their formation energies with V_H been lowest following this sequence: $E_{form}(V_H) < E_{form}(V_{CH}) < E_{form}(V_{C-CH}) < E_{form}(V_{C-C}) < E_{form}(V_C)$. The formation energies for the V_H and V_{CH} vacancies agree very well with those created in a single layer *graphane*. Nonetheless, in the -1 charge state, these defects might not be easily detected under moderate experimental conditions.

Fig. 2 depicts the calculated formation energies of the considered vacancy configurations as a function of Fermi level. We only present the formation energy plots of the most stable charge state. This plot also gives the thermodynamic transition levels given by the two lines intersecting shown in Fig. 2. In Fig. 2, it is evident that the V_H vacancy has the lowest formation energy while the V_C has the highest for the entire plot irrespective of charge state. The thermodynamic transition levels of all the vacancies occur at the top part of the band gap towards the CBM, indicating that our systems have the efficiency of the unpaired electrons in general. The V_H and

V_C have only the deep donor level (0/+1) at E_v+2.79 eV and E_v+3.29 eV respectively. It will not be easy to ionize such kind of the vacancies at room temperatures. For V_{CH}, the +1 charge state is stable for the entire band gap and overlaps with the charge states of other vacancy configurations. This suggests that, experimentally, the bilayer *graphane* containing these vacancy configurations at +1 charge state can exists after been annealed up to higher temperatures. Using the experimental methods such as perturbed angular spectroscopy (PAC) and deep level transient spectroscopy (DLTS), a peak corresponding to (0/+1) belonging to V_H and V_C should be noted, while for V_{CH} nothing is expected. Fig. 2 shows that divacancies V_{CH-C} and V_{C-C} posses both the donor (0/+1) and acceptor (-1/0) levels within the band gap. Eventhough these noted levels are deep, V_{CH-C} possesses acceptor (-1/0) level at E_c-0.21 eV which can easily be ionized. Although there are no available experimental data to compare with our values, we expect the experiments to record the two peaks or broad peak associated to donor (0/+1) and acceptor (-1/0). Since HSE06 functional and correction methods give better transition level positions in a band gap material [34, 35], we suggest the charged structure to be plausible requiring further experimental synthesis and characterization.

3.3. The electronic properties

Fig. 3 presents the total density of states (DOS) of pristine diamond-like bilayer *graphane* structure. In agreement with the previous studies [15, 17], this structure is a wide band gap semiconductor with non-spin polarized DOS for the entire plot. The band gap of 4.23 eV using HSE06 has been measured from Fig. 3.

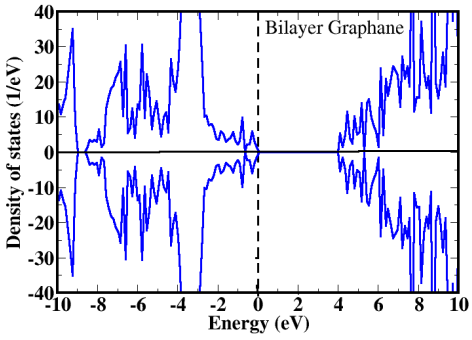

Figure 3: The total density of states of the diamond-like bilayer *graphane*. The position of Fermi level is at 0.00 eV and marked by black dashed vertical line.

The effects of the vacancies on the electronic properties of bilayer *graphane* are investigated using the density of states plots shown in Fig. 4. To calculate the magnetic moments arising from the difference between the spin up and spin down states, the majority and minority density of states are plotted. Fig. 4 also presents the influence of charge states (-1, 0, +1) modulation on the density of states of the identified vacancies.

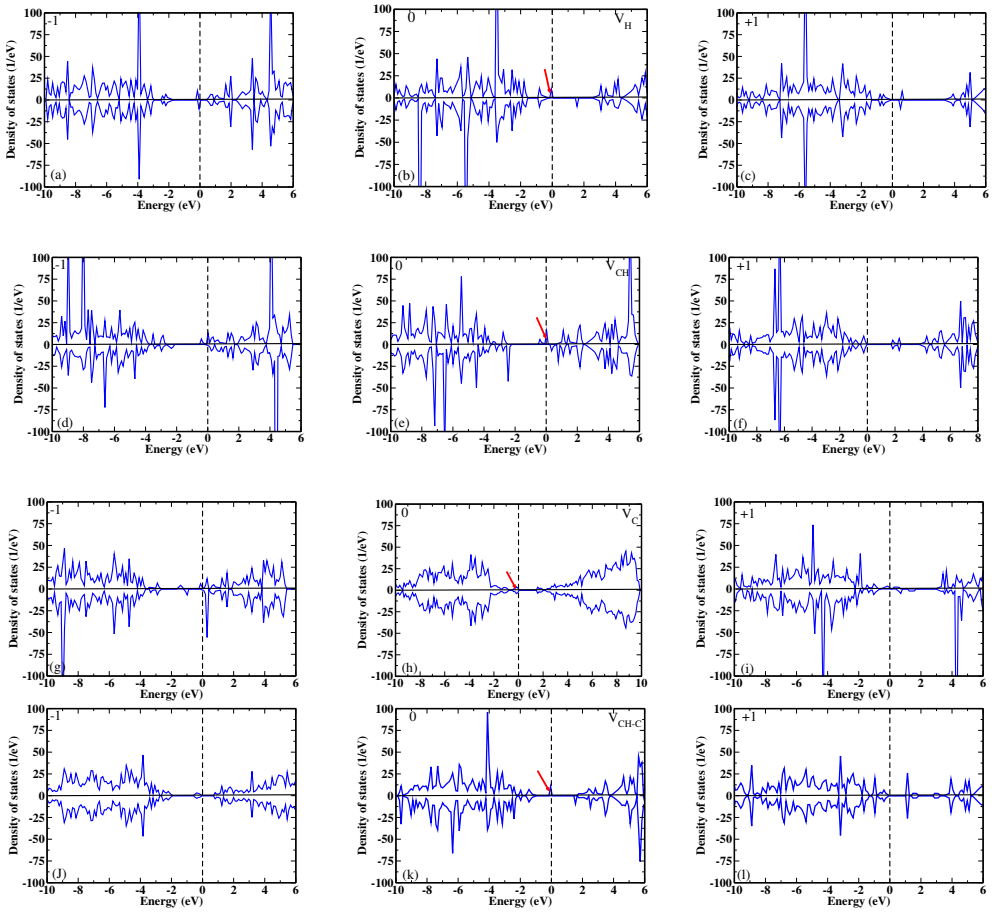

Figure 4: The calculated spin polarized total density of states of V_H at charge states (a) -1, (b) 0, (c) +1; V_{CH} at charge states (d) -1, (e) 0, (f) +1 ; V_C at charge states (g) -1, (h) 0, (i) +1 and V_{C-CH} at charge states (j) -1, (k) 0, (l) +1. The position of Fermi level is at 0.00 eV. The additional states introduced within the band gap (compared with the pristine case in Fig. 3) are vacancy induced states, indicated by the red arrow for each vacancy.

Fig. 4 shows that the V_H, V_{CH} and V_C vacancies introduce both the spin-up and spin-down states within the band gap of bilayer *graphane*. The states are mainly induced by atomic dangling bonds due to the removal of

their nearest neighbor native atoms, either H or C atom. The position and alignment of the induced states differ with vacancy configurations. For V_H, we see the spin-up states crossing the Fermi level around the mid band gap shown in Fig. 4(b), suggesting a metallic behavior.

Table 2 depicts that the V_H vacancy induced states are responsible for the total magnetic moment of $1.00\mu_B$ at 0 charge state. This was previously noted in a single layer *graphane*, and it was reported that an isolated H vacancy represents an unpaired electron in the dangling bond extending from the carbon atom, producing a magnetic moment of $1.00\mu_B$ [20, 17, 36]. For -1 (+1) charge state introduced in V_H, the Fermi level shifts up (backwards) towards the CBM (VBM), the spin-up and spin-down states are almost symmetrical for the entire plot, except at the vicinity of the Fermi level. At the Fermi level, the -1 charge state makes the spin-up states peak to be seen slightly below while the spin-down states peak crosses Fig. 4(a). Elias et al.[2] using experimental methods reported that *graphane* doped by electrons shift the Fermi level to reach the bottom of the conductance band in the hydrogenated region. In the +1 charge state, the Fermi level is noted between the vacancy induced non-spin polarized occupied states and slightly spin polarized empty states within the band gap shown in Fig. 4(c). The splitting of the induced spin up and down empty states yields the reduced magnetic moment of about $0.05\mu_B$ (see Table 2), suggesting that addition (-1) or removal (+1) of charge state saturates the V_H induced dangling bond.

The DOS of V_{CH} shown in Fig. 4(f) shows the induced partially occupied states crossing the Fermi level near the CBM, indicating the efficiency of dangling electron bonds in the system. The V_{CH} induces the magnetic moment of 1.00 μ_B (See Table 2) arising mainly from the partially occupied spin-up states. For the -1 charge state, the Fermi level is still noted closer to the CBM crossed by the partially occupied spin-up states. We suggests that an added electron also populates at the vicinity of the Fermi level resulting in the increment in the induced total magnetic moment to 1.50 μ_B. The effects of +1 charge state into V_{CH} vacancy reconstruct the DOS whereby the spin-up and spin-down states are symmetrical for the entire plot, revealing a non-magnetic nature. Interestingly, the Fermi level is seen just on top of the occupied non-magnetic VBM states, indicating a semiconductor character with a band gap of 1.74 eV. Saturating the vacancy induced dangling bond through charge state removal (+1) destroys the magnetic moment but retaining the non-magnetic states within the band gap, while hydrogen addition at the dangling bonds eliminate the induced states within the band gap of pristine *graphane*.

The V_C in a neutral state is non-magnetic because the spin-up and spin-down states are symmetrical for the entire plot including the vacancy induced

Table 2: The effects of charge states (-1, 0, +1) on the vacancy induced magnetic moment $m(\mu_B)$.

Vacancies	Charge states		
	-1	0	+1
V_H	0.05	1.00	0.05
V_{CH}	1.52	1.020	0.02
V_C	0.50	0.00	1.0
V_{C-CH}	0.30	1.00	0.00
V_{C-C}	0.00	0.00	0.00

occupied states at the vicinity of the Fermi level, suggesting the deficiency of dangling electron bonds in the system. This could be attributed to the induced electron bonding reconstruction mechanism during structural relaxation. The V_C vacancy in bilayer *graphane* shows the semiconducting features with a band gap of 1.40 eV. The -1 (+1) charge state into V_C rearranges the DOS, yielding the induced spin polarized states within the band gap with the Fermi level shifting backwards to the VBM (forward to the CBM) inducing the magnetic moment of 0.50 μ_B (1.00 μ_B). Fig. 4(k) reveals that the divacancy V_{C-CH} is metallic nature with induced partially occupied states crossing the Fermi level in a spin up channel. This yields a magnetic moment of 1.00μ_B. Just like in single vacancy the injection of -1 charge state in Fig. 4(j) (+1 charge state in Fig. 4(l)) suppresses this induced magnetic moment by shifting the Fermi level to the CBM (VBM). In conclusions, these vacancies studies induces more occupied and unoccupied states in different positions within the band gap which can be easily accessible through electronic tunneling which is the mechanisms requiring low temperature.

4. Conclusions

Using the *ab-initio* DFT calculations, we investigate the electronic structure of various possible vacancies (V_H, V_{CH}, V_C, V_{C-CH} and V_{C-C}) in a diamond-like bilayer *graphane* structure. It is noted that thermodynamic stabilities depend on the vacancy configurations and charge states modulation. These vacancies can be achieved using experimental pathways such as high-energy ion beams, the method used to create vacancies in a single layer graphene. In the +1 charge state, all the configurations are more stable suggesting that the dangling bonds extending from the C atoms around the vacancy in the neutral states are not desirable for room temperature device applications. For the thermodynamic transition levels analysis, it is suggested that these vacancies could be too deep in the band gap to be ionized.

For the electronic properties analysis of the vacancies in the various charge states, the density of states were plotted. In the neutral charge states, the vacancies induce the in-gap states responsible for the magnetic moment of 1.00 μ_B. The +1 charge state saturates the dangling bonds around the vacancy resulting in suppressing the magnetic moment and leading to non-spin polarized systems. The charge state modulation dependent properties in a diamond-like bilayer *graphane* structure is in agreement with the previous experimental studies in a single layer *graphane*. Our studies demonstrate that the vacancies in a diamond-like bilayer *graphane* structure could have potential applications in nanoelectronics and band gap related energy storage devices.

Acknowledgment

The authors acknowledges the University of Pretoria for financial support and computational resources. Prof Nithaya Chetty expresses gratitude to the National Institute for Theoretical Physics (NiThep) for funding.

References

[1] J. O. Sofo, A. S. Chaudhari, and G. D. Barber, *Phys. Rev. B*, **75**, 153401 (2007).

[2] D. C. Elias, R. R. Nair, T. M. G. Mohiuddin, S. V. Morozov, P. Blake, M. P. Halsall. A. C. Ferrari, D. W Boukhvalov, M. I. Katsnelson, A. K. Geim, and K. S. Novoselov, *Science*, **323**, 610 (2009).

[3] R. R. Nair, W. Ren, R. Jalil, I. Riaz, V. G. Kravets, L. Britnell, P. Blake, F. Schedin, A. S. Mayorov, S. Yuan, M. I. Katsnelson, H-M. Cheng, W. Strupinski, L. G. Bulusheva, A. V. Okotrub, I. V. Grigorieva, A. N. Grigorenko, K. S. Novoselov, and A. K. Geim, *small*, **6**, 24, 2877-2884 (2010).

[4] H Sahin and S Ciraci *Jour. Phys. Chem. C*, **116** 45, 24075-24083 (2012).

[5] P. R. Wallace, *Phys. Rev.*, **71**, 622 (1947).

[6] K. S. Novoselov, A. K. Geim, S. V. Morozov, D. Jiang, Y. Zhang, S. V. Dubonos, I. V. Grigorieva, and A. A. Firsov, *Science*, **306**, 666 (2004).

[7] K. S. Novoselov, A. K. Geim, S. V. Morozov, D. Jiang, Y. Zhang, M. I. Katsnelson, S. V. Dubonos, I. V. Grigorieva, and A. A. Firsov, *Nature (London)*, **438**, 197 (2005).

[8] K. S. Novoselov, Z. Jiang, Y. Zhang, S. V. Morozov, H. L. Stormer, U. Zeitler, J. C. Maan, G. S. Boebinger, P. Kim, and A. K. Geim, *Science*, **315**, 1379 (2007).

[9] J. Zou, L. Tang, K. Chen, and Y. Feng, *Jour. Phys.: Condens. Matter*, **30**,065001 (2018).

[10] Y. Cai, Q. Ke, G. Zhang, B. I. Yakobson, and Y.-W. Zhang, *Jour. Am. Chem. Soc.*, **138**, 10199-10206 (2016).

[11] A. A. Kistanov, Y. Cai, K. Zhou, S. V. Dmitriev, and Y.-W. Zhang, *Nanoscale*, **10**, 1403 (2018).

[12] D. W. Boukhvalov, M. I. Katsnelson and A. I. Lichtenstein, *Phys. Rev. B*, **77**, 035427 (2008).

[13] D. W. Boukhvalov and M. I. Katsnelson, *Phys. Rev. B*, **78**, 085413, (2008).

[14] F. Karlicky, R. Zboril and M. Otyepka, *J. Chem. Phys.*, **137**, 034709, (2012).

[15] O. Leenaerts, B. Partoens, and F. M. Peeters,*Phys. Rev B*, **80**, 245422 (2009).

[16] R. E. Mapasha, A. M. Ukpong, and N. Chetty, *Phys, Rev B*, **85**, 205402 (2012).

[17] R. E. Mapasha, M. P. Molepo and N. Chetty, *Phys. E.*, **79**, 52-58 (2016).

[18] J. Berashevich and T. Chakraborty, *EPL*, **93,** 47007 (2011).

[19] B. Dlubak, P. Seneor, A. Anane, C. Barraud, C. Deranlot, D. Deneuve, B. Servet, R. Mattana, F. Petroff and A. Fert, *Appl. Phys. Lett.*, **97**, 092502, (2010).

[20] H. Sahin, C. Ataca, and S. Ciraci, *Appl. Phys. Lett.*, **95**, 222510, (2009).

[21] J. Berashevich and T. Chakraborty, *EPL*, **93**, 47007, (2011).

[22] B. S. Pujari and D.G. Kanhere, *J. Phys. Chem. C*, **113**, 21063, (2009).

[23] J. Berashevich and T. Chakraborty, *Phys. Rev. B*, **82**, 134415,(2010).

[24] A. A. Kistanov, Y. Cai, K. Zhou, S. V. Dmitriev, and Y-W Zhang, *2D Mater*, **4**, 015010, (2017).

[25] RE Mapasha, MP Molepo, N Chetty, *RSC Adv.*, **7**, 63, 39748-39757, (2017).

[26] G. Kresse and J. Hafner, *Phys. Rev. B*, **47**, 558 (1993).

[27] P. E. Blochl, *Phys. Rev. B*, **50**, 17953 (1994).

[28] J. Heyd, G. E. Scuseria, and M. Ernzerhof, *J. Chem. Phys.*, **118**, 8207 (2003); **124**, 219906 (2006).

[29] H. J. Monkhorst and J. D. Pack, *Phys. Rev. B*, **13**, 5188, (1976).

[30] H.-P. Komsa, N. Berseneva, A. V. Krasheninnikov, R. M. Nieminen, *Phys. Rev. B*, **4**, 031044, (2014).

[31] J.-Y. Noh, H. Kim, and Y.-S. Kim, *Phys. Rev. B*, **89**, 205417 (2014).

[32] L. A. Openov, and A. I. Podlivaev, *Semiconductors*, **52**, 6, 760-765 (2018).

[33] Jin C, Lan H, Peng L, Suenaga K, Iijima S. *Phys Rev Lett*, **102** 205501 (2009).

[34] A. Janotti and C. G. Van de Walle, *Phys. Status Solidi B*, **248**, 799 (2011).

[35] H. -P. Komsa and A. Pasquarello, *Phys. Rev. B*, **84**, 075207 (2011).

[36] C. -K. Yang, *Carbon*, **48**, 3901 (2010).